Kaylor *et al. Movement Ecology* (2025) 13:6
https://doi.org/10.1186/s40462-024-00524-3

Movement Ecology

RESEARCH **Open Access**

Watershed-scale dispersal patterns of juvenile Chinook Salmon (*Oncorhynchus tshawytscha*) revealed through genetic parentage analysis

Matthew J. Kaylor[1*], Lindsy R. Ciepiela[2], Melody Feden[2], Joseph T. Lemanski[2], Casey Justice[1], Benjamin A. Staton[1], Jonathan B. Armstrong[3], Stefan Kelly[4], Shawn R. Narum[5], Ian A. Tattam[2] and Seth M. White[3]

Abstract

Background For many aquatic taxa, juvenile dispersal from spawning locations to rearing habitats is a critical process influencing individual fitness and population dynamics. However, our understanding of dispersal patterns in naturally spawning fish populations remains largely unknown due to the logistical challenges of tagging and tracking movement at early life stages.

Methods We quantified dispersal patterns of a spring-run Chinook Salmon (*Oncorhynchus tshawytscha*) population in NE Oregon, USA using genetic parentage-based tagging to trace juveniles captured from summer rearing habitats back to their maternal parent and associated spawning location (i.e., juvenile origin). We evaluated overall dispersal patterns, longitudinal trends across the watershed, and relationships between dispersal and biophysical factors, including thermal conditions, network-scale abundance estimates, and juvenile size-at-capture.

Results Overall dispersal of the 1326 juveniles (n sampled = 3388) assigned to a maternal parent (n = 64) was downstream-biased, but we estimated that 32% dispersed upstream and 29% moved into adjacent tributaries after initial mainstem dispersal. Dispersal distances were high relative to those found in other studies, with 25% of parr dispersing more than 0.9 km upstream (max = 10.6 km) and 25% dispersing more than 3.7 km downstream (max = 28.6 km). Analysis of dispersal patterns and potential drivers indicated that (1) dispersal distances, directional bias, and variability showed clear longitudinal trends from downstream to upstream origin locations, (2) temperature was a dominant driver of dispersal, with individuals originating from warmer sections of the mainstem typically moving to cooler mainstem sections or tributaries, and (3) dispersal distance was associated with larger size-at-capture for individuals that dispersed downstream, but not upstream.

Conclusions The widespread dispersal patterns exhibited in this population, including moving considerable distances upstream, downstream, and into tributaries, suggests that dispersal in naturally spawning fish populations may be more extensive and variable than currently recognized. We found that heterogeneity in biophysical conditions shaped within-population variability and riverscape dispersal patterns with important implications for subsequent fish habitat use, distribution, and size. This study provides an approach to evaluate patterns and drivers of dispersal

---

*Correspondence:
Matthew J. Kaylor
mkaylor@critfc.org

Full list of author information is available at the end of the article

in naturally spawning populations and inform conservation and restoration planning through better alignment with juvenile fish ecology.

Keywords Chinook salmon, Dispersal, Riverscape patterns, Genetics, Habitat complementation, Habitat use, Thermal refuge, Fish distribution, Parentage-based tagging

Background

Variation in physical habitat conditions, food resources, and biotic interactions (e.g., competition, predation) form dynamic landscapes of habitat quality [1] that shape individual and population-level fitness [2, 3]. As this mosaic of landscape conditions shifts, movement allows animals to seek favorable habitats that enhance individual fitness; for example, by reducing competition [4, 5], avoiding sub-optimal or lethal environmental conditions [6, 7], and tracking food resources and thermal conditions to maximize growth opportunities [8–10]. Evaluating movement amongst this complexity is challenging, and rivers have served as model ecosystems to evaluate movement patterns in fish and other mobile aquatic organisms as movement is confined within stream channels. The ability to tag and track individual fish has produced a large body of work advancing our understanding of riverine fish movement [11–13]; however, movement patterns vary across life stages [14] and comparatively few studies have evaluated movement patterns in early life stages of wild fish populations (but see [14–16]) due to constraints of traditional tagging and tracking approaches. This leaves a knowledge gap in our understanding of individual- and population-level movement patterns for early life stages of wild fish populations, including how variability in biophysical conditions across watersheds may structure movement patterns.

The combined active (i.e., swimming independent of current) and passive (i.e., downstream drift with water current during early life stages) movement of juvenile salmon from spawning nests (redds) to rearing habitats, hereafter referred to as “dispersal”, is a critical process affecting individual growth and survival [17], which collectively influences population dynamics through effects on juvenile distribution, habitat utilization, and production [18, 19]. Anadromous salmon are highly fecund and their spawning locations are often clustered at both small (e.g., multiple redds within a pool tail-out) and large (i.e., core reaches within a basin) spatial scales [20], resulting in high localized densities of recently emerged juveniles [21]. Juveniles that disperse to lower-density habitats typically exhibit greater growth and subsequent survival [17, 22, 23], and collectively, these individual dispersal patterns can influence population-level density-dependent effects. Further, spatial patterns in juvenile rearing habitat quality may not align with spawning distributions, and dispersal facilitates juvenile habitat selection and rearing range expansion, including into tributaries and headwaters not used by spawning adults [15, 24]. However, the spatial distribution of juvenile salmonids often mirrors adult spawning distributions [25, 26], suggesting limited overall dispersal, or alternatively, that spawning and rearing habitat are supplementary.

Empirical evaluations of juvenile salmon dispersal generally suggest that movement after emergence from redds to rearing habitat is limited (< 0.5 km of origin) and biased downstream [27], conforming with the Restricted Movement Paradigm (RMP; [11]) which postulates that most individuals in a population are sedentary during nonmigratory periods. However, unbiased and accurate dispersal estimates are limited and there is increasing evidence challenging the RMP in juvenile salmon as dispersal is evaluated across a wider range of environmental conditions [27]. The majority of studies evaluating early life-stage salmonid dispersal have done so by outplanting embryos or fry to streams (reviewed by Eisenhauer et al. [27]), typically at small spatial scales and with low variability in biophysical conditions. Reducing variability is often necessary to test specific hypotheses and these studies have greatly informed our understanding of factors influencing dispersal [17, 22, 28]; however, few studies have evaluated dispersal in naturally spawning populations (but see [14, 15]).

Wild populations are exposed to greater variability in inter- and intra-specific competition, environmental conditions, habitat quality, and emergence timing [29], likely stimulating variable dispersal patterns across watersheds. Indeed, studies evaluating juvenile salmonid dispersal in naturally spawning populations have reported large-scale dispersal of tens or hundreds of kilometers associated with alternative life-history strategies [24, 30]. We currently lack an understanding of dispersal at finer spatial scales (i.e., within natal rearing extents) and to our knowledge, no studies have evaluated population-level dispersal across the entirety of the adult spawning and juvenile rearing extents. This represents a fundamental knowledge gap, as dispersal largely dictates how landscape configuration (i.e., the spatial arrangement of habitat patches) affects early life stages of freshwater fish. Understanding these patterns and the mechanisms that drive them has important implications for prioritizing the types and locations of management efforts to maximize habitat use and benefit to juvenile salmonids.

In this study, we used a riverscape sampling approach and genetic parentage-based tagging (PBT) to quantify juvenile dispersal patterns of a wild population of spring-run Chinook Salmon in NE Oregon, USA. Additionally, we estimated parr abundance and distribution across the river network to relate spawning and dispersal patterns to parr distribution and to correct for sampling bias effects on our inference into population-level dispersal. Our objectives were to: (1) characterize overall dispersal patterns of a naturally spawning population; (2) evaluate spatial variability in dispersal patterns across the watershed, including potential drivers of observed patterns; and (3) assess how dispersal distance and direction (upstream vs. downstream), and other biophysical factors (e.g., temperature, emergence timing, density) relate to parr length-at-capture.

Methods

Study area and species description

The study was conducted in the Middle Fork John Day River (MFJDR), a tributary of the John Day River in northeast Oregon. The MFJDR watershed encompasses 2051 km^2 and flows northwest from its origins in the Blue Mountains to its confluence with the North Fork John Day River (Fig. 1). The study area is approximately 700 river kilometers (rkms) from the Columbia River estuary (subsequent rkm measurements are relative to the mouth of the MFJDR) and anadromous fish encounter three dams on the mainstem Columbia River en route to and from spawning grounds in the MFJDR. The region is characterized by hot summers with little precipitation and cold winters in which most of the precipitation is snow. Streamflow peaks during spring snowmelt – typically March to May – and is lowest during mid-to-late summer, a period coinciding with maximum water temperature. The timing of spring snowmelt and the onset of summer low flow conditions occurred early in 2021, and mainstem flows for the first week of July and August were 56% (28.5 cfs) and 75% (15.7 cfs), respectively, of 2012–2020 (period of record) average discharge (USGS gauge 14043840).

Spring-run Chinook Salmon in the MFJDR spawn throughout September with most spawning occurring between rkms 80–115 of the mainstem [31]. Embryos incubate throughout the fall and winter, with emergence generally occurring between March and May; however, emergence occurs earlier in upstream reaches where winter water temperatures are warmer [29]. During the summer rearing period, stream thermal conditions largely restrict parr rearing to mainstem habitats and adjacent tributaries located upstream of rkm 80. However, low parr densities have been observed in several small tributaries between rkms 60–80 and within the mainstem in cooler summers with higher flow (M. Kaylor unpublished data). As summer rearing transitions into winter-rearing, parr exhibit two main life history strategies: (1) fall-migrants leave summer rearing reaches to overwinter in larger mainstem habitats downstream and (2) spring-migrants overwinter in natal mainstem and tributary habitats overlapping the summer rearing extent. Both fall- and spring-migrants spend approximately one year in the stream following emergence before smoltification and downstream migration to the estuary in spring [31, 32]. The John Day basin has no history of hatchery supplementation and hatchery adult strays into the basin are rare.

In addition to spring-run Chinook Salmon, the fish community in the MFJDR is comprised of steelhead/rainbow trout (*O. mykiss;* the only other anadromous salmonid), mountain whitefish (*Prosopium williamsoni*), northern pikeminnow (*Ptychocheilus oregonensis*), redside shiner (*Richardsonius balteatus*), bridgelip sucker (*Catostomus columbianus*), largescale sucker (*Catostomus macrocheilus*), speckled dace (*Rhinichthys osculus*) and sculpin (*Cottus spp.*) [33].

Adult sampling

We sampled adult Chinook Salmon in September 2020 during the peak of spawning activity (9/16/2020–9/23/2020). Surveyors (1–2 individuals per reach) walked the entire length of the spawning distribution on 9/16/2020 and 9/21/2020, collecting tissue samples from carcasses, recording redd locations, and noting locations of live adults using standard spawning ground survey techniques [31]. We supplemented standard surveys with intensive daily surveys conducted by a smaller group of 2–4 surveyors, targeting locations of live adults. During both standard and intensive surveys, we examined carcass body cavities to determine sex and spawn completeness, and we collected an operculum tissue sample (occasionally fin or heart tissue when operculum was degraded or not present). Tissue samples were pressed onto Whatman paper, inserted in paper coin envelopes, air-dried, and stored until genetic processing.

Parr sampling

We selected parr sampling sites to achieve a spatially balanced distribution throughout the core rearing range of the mainstem (rkms 79–118) and associated tributaries (Fig. 1; Table 1). Prior to parr sampling, we selected 30 mainstem sites: 10 sites were part of on-going research by Oregon Department of Fish and Wildlife (ODFW) and Confederated Tribes of the Warm Springs Reservation of Oregon (CTWSRO), and 20 sites were selected from an existing Columbia Basin-wide Generalized Random Tessellation Stratified sample [34]. However, parr were either not present or in too low abundance to sample at nine planned mainstem sites (rkms 80–90 and 111–113), resulting in 21 sampled mainstem sites. Given the potential importance of cool- and cold-water tributary use, we also sampled parr from nine tributaries. We

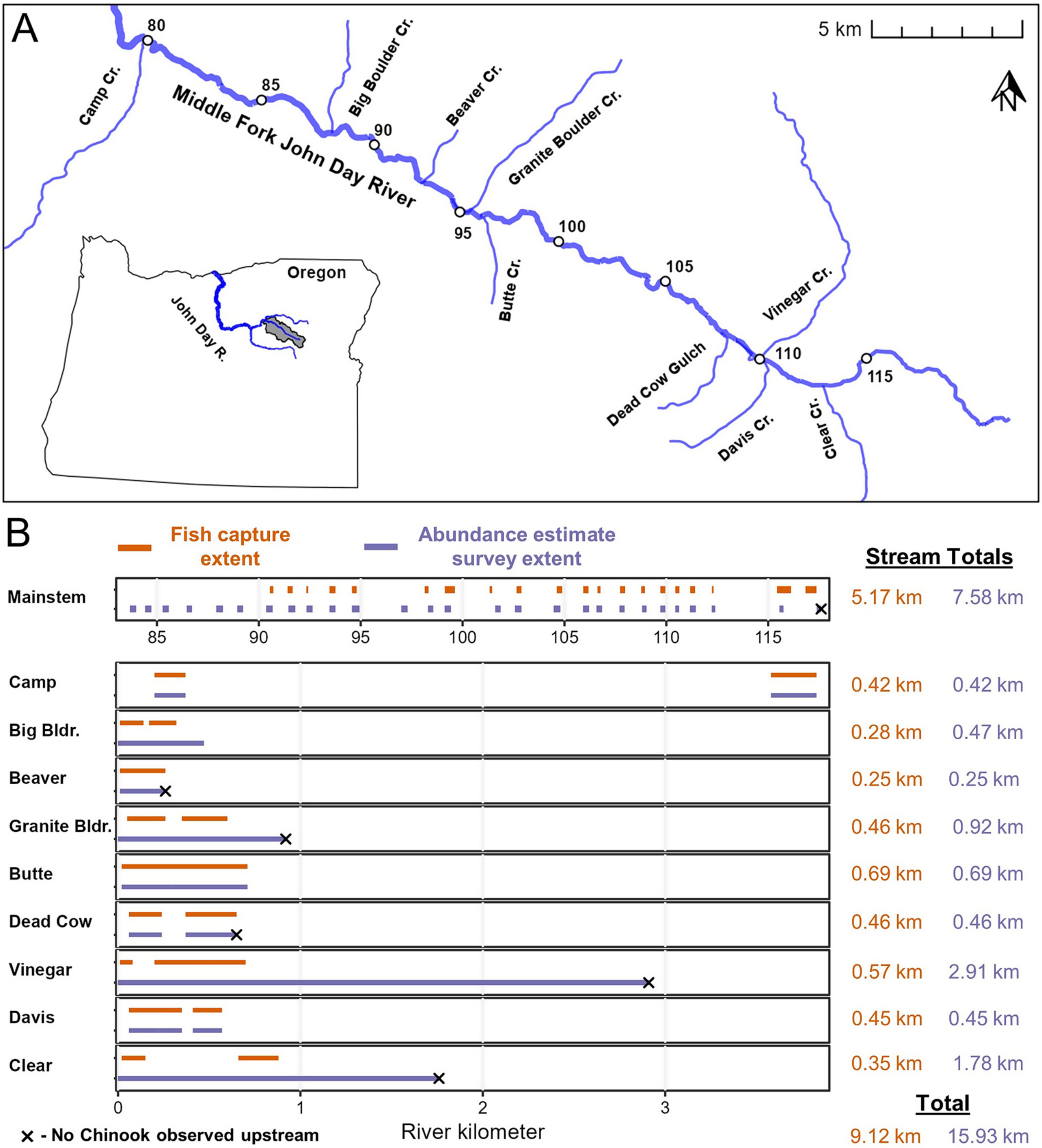

Fig. 1 (**A**) Extent of sampling conducted in the MFJDR (rkm indicated by open points) and nine sampled tributaries. (**B**) The location of parr capture sampling (orange) and abundance estimate surveys (purple) with the right column listing the total stream length sampled by each method. Black x's indicate the upstream extent of parr distribution, while the absence of an x indicates sampling did not occur upstream of this location due to property access or other sampling constraints. Mainstem capture sampling was planned between rkms 80–90 but not conducted after snorkel surveys revealed that parr densities were too low to feasibly sample

Table 1 Mainstem and tributary characteristics and fish sampling details

Stream	Rkm	Mean width (m)	July Q (L s^{-1})	July MDMT (°C)	Parr sampling			
					Dates sampled	*n* sampled	*n* paired to female	Mean fork length (mm)
Mainstem	-	7.4	596.0	21.8–26.2	7/13–8/9	1592	595	67.3
Camp Cr.	79.8	3.4	12.2	21.3	7/9	28	13	60.0
Big Bldr Cr.	88.1	4.7	70.9	23.1	7/1,7/2	184	93	57.7
Beaver Cr.	92.8	1.4	21.3	19.6	7/14	63	12	62.2
Granite Bldr Cr.	95.1	4.4	124.3	17.5	6/30,7/22	292	80	68.3
Butte Cr.	96.4	2.5	4.1	18.8	7/14,7/20	248	70	61.1
Dead Cow Gu.	108.3	2.4	-	19.0	7/8,7/9	182	93	62.3
Vinegar Cr.	110.0	3.4	-	21.4	6/29–7/22	399	172	59.6
Davis Cr.	110.7	1.8	-	23.3	7/6,7/8	200	115	62.2
Clear Cr.	112.8	4.3	132.4	20.7	7/7,7/22	200	83	65.8
Total	-	-	-	-	6/29–8/9	3388	1326	64.7

incorporated samples from two reaches in Vinegar Creek and one reach in Camp Creek that were part of ongoing research by ODFW. We selected the remaining sampling reaches within tributaries to maximize spatial coverage of salmonid rearing habitat while accommodating time constraints dictated by stream temperatures and land ownership.

We sampled parr between 6/29/2021 and 8/19/2021, during summer rearing and prior to downstream movement associated with winter-rearing or outmigration. Based on predicted median emergence timing between 4/6/2021 and 5/10/2021 (Additional File 1: Fig. S1; [29]), parr sampling occurred approximately 3–4 months post-emergence. Tributaries were generally sampled earlier than mainstem sites (Table 1), as warmer mainstem temperatures prohibited sampling for much of July. We captured parr using snorkel seining methods (snorkelers visually identified Chinook Salmon parr and herded them into a 1.8 m x 4.6 m seine net) except for in five shallow tributaries which we sampled with backpack electroshockers (Smith Root LR-20B). At each site, we navigated to a pre-determined GPS point and then progressed upstream. Parr from individual habitat units (e.g., a single pool) were kept in separate, labeled buckets and unit-specific GPS points were taken. We sampled a maximum of 25 parr from individual habitat units to ensure that we sampled from multiple units within each site. In smaller tributaries with low parr abundance, we combined parr from multiple units into composite units not exceeding 50 m in length. Captured parr were anesthetized using an Aqui-S 20E concentration of 20 mg/L, measured (fork length, nearest mm) and weighed (nearest 0.1 g). Small, non-lethal, caudal fin clips were pressed onto gridded Whatman paper, air-dried, and stored in paper folders for genetic processing. We allowed parr to recover in aerated buckets and then released them into the unit they were sampled from.

Genotyping

Tissue samples from adults and parr were genotyped to enable parentage analyses. DNA was extracted from tissue samples using the Chelex 100 method, and then DNA libraries of barcoded individuals were prepared and sequenced following the genotyping-in-thousands method (GTseq; [35]) with one round of polymerase chain reaction to amplify targeted genetic loci and another to add barcodes to identify individuals. Each sample was then normalized and pooled into a sequencing library. The library was quantified and then sequenced using an Illumina NextSeq 2000 instrument. The GTseq panel included 354 single nucleotide polymorphisms (SNPs), with a subset of 254 putatively neutral markers intended for parentage analyses along with a genetic sex marker to verify males vs. females (see Hess et al. [36] for details). All samples and genetic markers with 10% or more missing SNPs were considered failed genotypes and were not retained for analyses. Because some sampled carcasses were too degraded or scavenged to accurately determine sex, we relied on genetic sex assignments for all adults.

Parentage assignments (i.e., parr-adult pairings) were performed using CKMRsim software [37] and Close-Kin Mark-Recapture methods [38] were used to estimate likelihoods between each adult and parr sample. We included pairwise relationships between parr and negative adult controls (adults originating outside the John Day River Basin), to assess the false positive and false negative rates expected for the adult-parr dataset and compared the log-likelihood ratio (LLR) distributions of MFJDR parentage assignments relative to negative control assignments to determine an LLR threshold. The LLR of negative control samples ranged from – 29 to -1, whereas MFJDR parent assignments exhibited a bimodal distribution, intersecting at an LLR value of approximately 12 (Additional File 1: Fig. S2). We applied a conservative LLR threshold of 20 and excluded parr-adult assignments with LLR lower than this value (false positive rate < 0.01). We only evaluated dispersal using parr-female pairs, as male carcass locations were not expected to provide reliable proxies of redds due to movement after spawning and spawning with multiple females [39].

Abundance estimates

We estimated parr abundance within sample reaches using snorkel and electrofishing surveys (Fig. 1; Table 2), and then used these estimates to predict parr abundance across unsampled portions of the MFJDR watershed. We snorkeled 27 mainstem reaches (total length = 7.58 km) and continuous sections of the four largest tributaries (6.08 km). We conducted electrofishing surveys in five tributaries that were too shallow to snorkel (2.27 km; Table 2).

Snorkel surveys were conducted at the habitat unit-level, in which snorkelers recorded counts of Chinook Salmon parr observed. For mainstem reaches, we progressed upstream until survey length exceeded 15x bankfull width (range: 174–388 m). In tributaries, we progressed upstream until no parr were observed in three consecutive pools and we assumed that parr abundance upstream of this point was negligible. The exception was Big Boulder Creek, in which surveys were concluded at a private property boundary ~ 500 m upstream from the confluence. We visually delineated habitat units as pools, fast-non-turbulent (FNT; i.e., runs, glides), and fast-turbulent (FT; i.e., riffles). We sampled all pools and FNTs but sampled alternating FTs in mainstem sites and every fourth FT in tributaries due to time constraints and lower counts observed in these habitats [40].

To adjust for imperfect detection in snorkel surveys, we measured unit-specific habitat attributes that can affect detection and applied the model developed by Staton et al. [41] to predict detection probability of each survey. These attributes included unit type, average depth, density of large wood pieces, and an observer-determined visibility index. For each unit ($n = 432$), we sampled 1000 detection probability values with replacement from the posterior predictive distributions given by Staton et al.'s [41] model and used them to expand the partial snorkel counts to a distribution of abundance estimates. We imputed abundance for skipped units using mean density from sampled units of that site and unit type. We then summed across all units for each iteration to obtain 1000 abundance and density estimates per mainstem reach or tributary.

For smaller tributaries, we conducted equal-effort, single-pass electro-fishing surveys (without block nets) in one to three reaches and enumerated all captured parr. We expanded counts to abundance estimates using reach-scale capture efficiency estimates obtained from ODFW using paired single-pass and mark-recapture surveys conducted in MFJDR tributaries between 2019 and 2021. For each unit, we simulated 1000 abundance estimates by drawing from the distribution of capture efficiencies (mean = 0.26; SD = 0.083), and we generated reach-scale estimates by summing across all units within each reach.

We generated reach-, stream-, and basin-wide abundance estimates by predicting abundance at unsampled locations. We created prediction sites ~ 300 m in length between surveyed sites and predicted parr density for each unsampled site (# m^{-1}) using linear interpolation of sampled sites. We generated 1000 density predictions for each site, which we then multiplied by reach length to obtain a distribution of abundance predictions. We assumed that mainstem abundance was zero downstream of rkm 83 and upstream of rkm 117, as surveys conducted beyond these points indicated few or no parr. Lastly, we summed abundance estimates across reaches for each iteration to obtain a distribution of stream-specific and whole-basin abundance estimates.

Sampling bias adjustments

Population-level dispersal patterns may be influenced by sampling bias if sampled parr do not represent a random sample of the population [42]. Ideally, the number of parr sampled at each site would be proportional to parr

Table 2 Summary of mainstem and tributary abundance ($\hat{N}$) and density estimates

Stream	Rkm	Method	$\hat{N}$	$\hat{N}$ 95% CI	% of total (95% CI)	Mean density (# m^{-1})	Max density (# m^{-1})
Mainstem	80–116	snorkel	49,096	45,149–54,937	72.6 (69.9–75.3)	1.27	4.85
Camp Cr.	79.8	e-fish	1054	727–2373	1.6 (1.1–3.4)	0.27	0.31
Big Bldr Cr.	88.1	snorkel	1151	1064–1258	1.7 (1.5–1.9)	2.38	3.34
Beaver Cr.	92.8	e-fish	256	181–479	0.4 (0.3–0.7)	1.03	1.03
Granite Bldr Cr.	95.1	snorkel	4254	3323–5813	6.3 (4.9–8.5)	5.16	11.37
Butte Cr.	96.4	e-fish	1064	848–1566	1.6 (1.3–2.3)	0.88	2.13
Dead Cow Gu.	108.3	e-fish	1110	859–1694	1.6 (1.3–2.4)	1.69	2.17
Vinegar Cr.	110.0	snorkel	4643	4400–4981	6.9 (6.2–7.5)	1.53	2.96
Davis Cr.	110.7	e-fish	1246	957–1954	1.8 (1.4–2.9)	1.63	2.81
Clear Cr.	112.8	snorkel	3485	3052–4025	5.1 (4.4–6.0)	2.11	4.12
Total	-		67,359	60,560–79,080	-	-	

abundance. This was logistically impractical as we did not have a priori abundance estimates and because abnormally warm temperatures in July prohibited mainstem sampling in some locations. To reduce sampling bias effects on dispersal inference, we calculated and assigned sampling weights to individual fish based on capture reach. Sampling weights were equal to the predicted proportion of the population located at each sampling reach (P_{pop}) divided by the respective reach sampling proportion (P_{samp}), where P_{pop} is equal to the mean predicted abundance at each reach divided by the predicted mean basin abundance (67753) and P_{samp} is equal to the reach sample size divided by the total sample size ($n = 3388$ parr). These weights therefore provide an estimate of the degree to which reaches were over- or under-sampled and were incorporated into models as weighting factors.

Temperature

To evaluate thermal conditions across the MFJDR in summer 2021, we used hourly water temperature data from loggers distributed across the watershed [43]. We downloaded data in fall 2021 from 38 mainstem locations (rkms 76–114) and all nine sampled tributaries, in which loggers were located within a kilometer upstream from the mainstem confluence. Temperature data were filtered through a standardized QAQC process and visually inspected for errors. We summarized daily mean and max temperature and calculated mean daily maximum temperature (MDMT) across the months of June ($\text{MDMT}_{\text{June}}$) and July ($\text{MDMT}_{\text{July}}$). All nine tributaries exhibited cooler temperatures compared to adjacent mainstem sections with the greatest differences occurring in Beaver Creek, Granite Boulder Creek, Dead Cow Gulch, and Clear Creek (Table 1; Additional File 1: Fig. S3).

Dispersal analyses

We calculated dispersal as the stream distance between each parr-female pair such that negative values indicated downstream mainstem dispersal (i.e., parr captured downstream of female parent) and positive values indicated upstream mainstem dispersal. Tributary distance was negative if the tributary confluence was downstream of the female location, and positive if upstream of females. Thus, negative dispersal values indicate directionality of mainstem dispersal, and for tributary dispersers, reflects the total distance dispersed including downstream mainstem and upstream tributary dispersal. We also present total distance moved regardless of direction as a response variable.

We first evaluated the overall distribution of all dispersal estimates including the median, inter-quartile range (IQR), and 95% quantiles. We calculated metrics using weighted quantiles, in which weights were proportional to the estimated sampling bias of reaches and were applied to all parr captured within that reach (described above). We evaluated both dispersal and total distance for all parr and stratified by parr that were captured within the mainstem versus tributaries.

We evaluated spatial patterns of parr dispersal across the MFJDR using two approaches: 1) we used a general linear mixed-effects model (GLMM) to predict mean dispersal as a function of parr origin rkm (i.e., rkm of paired female), and 2) we evaluated dispersal at a finer-scale by grouping parr into sections based on their origin and plotting where they dispersed to using weighted density distributions. Dispersal distance was the response variable with model fit providing an estimate of upstream vs. downstream dispersal bias. We fitted the model with an interaction between origin rkm and an indicator variable for whether parr were captured within the mainstem or tributaries and we included sampling bias weights applied to individual parr. To account for potential correlation in dispersal patterns among related individuals, we included the unique identifier of female parents as a random effect in which all offspring from an individual female had the same random effect identifier. We fitted separate models with parr origin rkm as a linear, 2nd order polynomial, and 3rd order polynomial relationship and assessed model fit using AIC_{c} [44] in which the 2nd order polynomial relationship had the most support. The relationship between model residuals and river kilometer indicated heteroscedasticity and we therefore modeled the residual standard error as having a linear relationship with origin rkm and the response variable using the R package 'glmmTMB' [45]. We used Moran's I test to assess whether residuals from our models showed problematic levels of spatial autocorrelation (implemented via the 'DHARMa' R package [46]), which revealed no evidence of residual spatial autocorrelation.

We used binary logistic regression to assess the influence of water temperature on dispersal of parr. We developed three binary variables (assigned 0 if condition not met, 1 if met), each coded depending on how the $\text{MDMT}_{\text{July}}$ value for the capture location of each parr differed from its origin location; the thresholds used were > 0.5 °C (i.e., moved to warmer location), < -0.5 °C, and < -2 °C (i.e., cooler locations). We fitted three independent logistic regression models with each binary variable as the response and the $\text{MDMT}_{\text{July}}$ value at the origin location as the sole fixed effect predictor variable; similar to other models we used, we included a random effect for the female parent identifier and used sample bias weights to weight each observation.

We used GLMMs to evaluate the relative contribution of spatial ecological factors (particularly dispersal distance) influencing parr size-at-capture while accounting for potential confounding effects of sampling date. Parr origin rkm was included because we expected parr size to exhibit spatial patterns independent of dispersal as emergence timing is longitudinally structured in the MFJDR [29], which can translate to longitudinal patterns of parr summer size [40]. Parr fork length was the response variable, and we included distance moved, parr origin rkm (2nd order polynomial), mainstem vs. tributary capture, dispersal direction (upstream vs. downstream), sampling day, max temperature ($\text{MDMT}_{\text{July}}$) of capture locations, and density at capture locations (parr m^{-1}) as fixed-effects, the unique identifier of the female parent as a random effect, and sample bias weights. To evaluate whether mainstem vs. tributary capture and dispersal direction were important factors describing size-dispersal relationships, we fitted each candidate model with different combinations of interactions and additive effects of these covariates. We assessed collinearity and removed models from the candidate set when the variance inflation factor exceeded 10 for one or more terms [47]. We used AIC_c to select a set of plausible models ($\Delta\text{AIC}_c < 2$) and then chose the model with the fewest parameters.

Results

Genotyping

We identified 161 redds across the mainstem MFJDR and a single redd in Clear Creek in September 2020 (Fig. 2; Additional File 1: Fig. S4), which is 60% of the 20-year mean of 272 redds. We sampled tissue from 141 individual spawners (41% of the estimated total spawners) and 113 of these samples were successfully genotyped (< 10% of SNPs missing), of which 67 were females and used in analyses. The distribution of redds generally mirrored the distribution of successfully genotyped females across the study extent, except rkms 90–100 (Additional File 1: Fig. S4) where genotyped females were relatively under-represented, and surveyors noted greater evidence of scavenging.

Of the 3388 sampled parr, 1326 (39.1%) were assigned to a maternal parent, of which 595 (44.9%) of the assigned parr were captured from mainstem sites and 731 (55.1%) from tributaries (Table 1). At least one parr was assigned to 64 of the 67 females retained after genotyping, but apparent reproductive success was not uniform as just 16 females accounted for approximately 50% of the parr assigned to females (Additional File 1: Fig. S5).

Abundance estimates

Total parr abundance estimated across the MFJDR was 67,359 (95% CI = 60560–79080), with the mainstem accounting for nearly three-quarters of all parr (Table 2). Among tributaries, total abundance estimates were greatest in Vinegar Creek, Granite Boulder Creek, and Clear Creek, accounting for 18.3% of total MFJDR basin

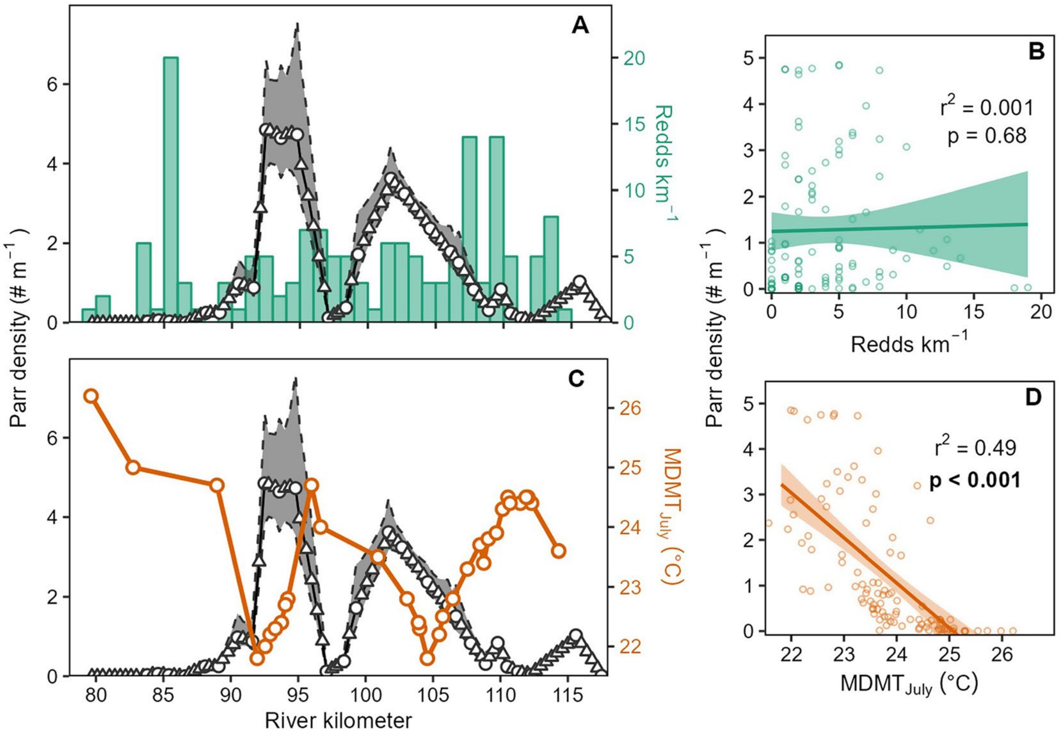

Fig. 2 (**A**) Spatial patterns of redds in 2020 (green bars) relative to mainstem parr density in summer 2021, and (**B**) the associated linear relationship. (**C**) Spatial patterns of temperature ($\text{MDMT}_{\text{July}}$; orange points and line) relative to mainstem parr density, and (**D**) the associated linear relationship. For density estimates in panels A and C, points represent snorkeled sites, triangles indicate prediction reaches, and grey shading between dashed lines show 95% confidence intervals

abundance, whereas the other six tributaries individually accounted for less than 2% of total parr abundance.

The highest estimated densities within the mainstem were rkms 91–96 and 100–106 (Fig. 2). These areas accounted for 28% of total redds observed in 2020 but 54% of total parr abundance (Fig. 2), suggesting net immigration into this reach. In contrast, 35% of redds were observed downstream of rkm 90 and upstream of rkm 110, but we estimated that just 6.4% of all parr occupied these areas, which suggests net emigration or high rates of mortality. Consequently, the distribution of redds was not well associated with mainstem parr density (*p* = 0.68; Fig. 2B). Mainstem parr density was inversely related to July maximum temperature ($\mathrm{MDMT}_{\mathrm{July}}$; Fig. 2C, D).

Sampling-bias weights suggested that we under-sampled most mainstem sites and over-sampled most tributaries (Additional File 1: Fig. S6). The mean sampling-bias weight for parr sampled from the mainstem was 1.47, indicating approximately 50% more parr should have been sampled to achieve sample sizes proportional to the estimated relative abundance of parr. In contrast, the mean sampling-bias weight for parr captured in tributaries was 0.51 (range: 0.21–1.89), indicating that we should have sampled around half as many parr.

Overall dispersal

Parr dispersal was downstream-biased (median = -0.77 km), and we estimated that 68% of parr dispersed downstream (Fig. 3A). Dispersal estimates varied widely (95% range: -14.9–6.2 km) and we estimated that 25% of parr dispersed farther than 3.7 km downstream and 25% dispersed at least 0.9 km upstream. Dispersal patterns differed for parr captured within the mainstem vs. tributaries (Fig. 3B, C): mainstem-captured parr exhibited downstream-bias (median = -1.4 km; 78% dispersed downstream) whereas dispersal was upstream biased for tributary-captured parr (median = 0.7 km; 57% dispersed upstream). The median estimated distance parr

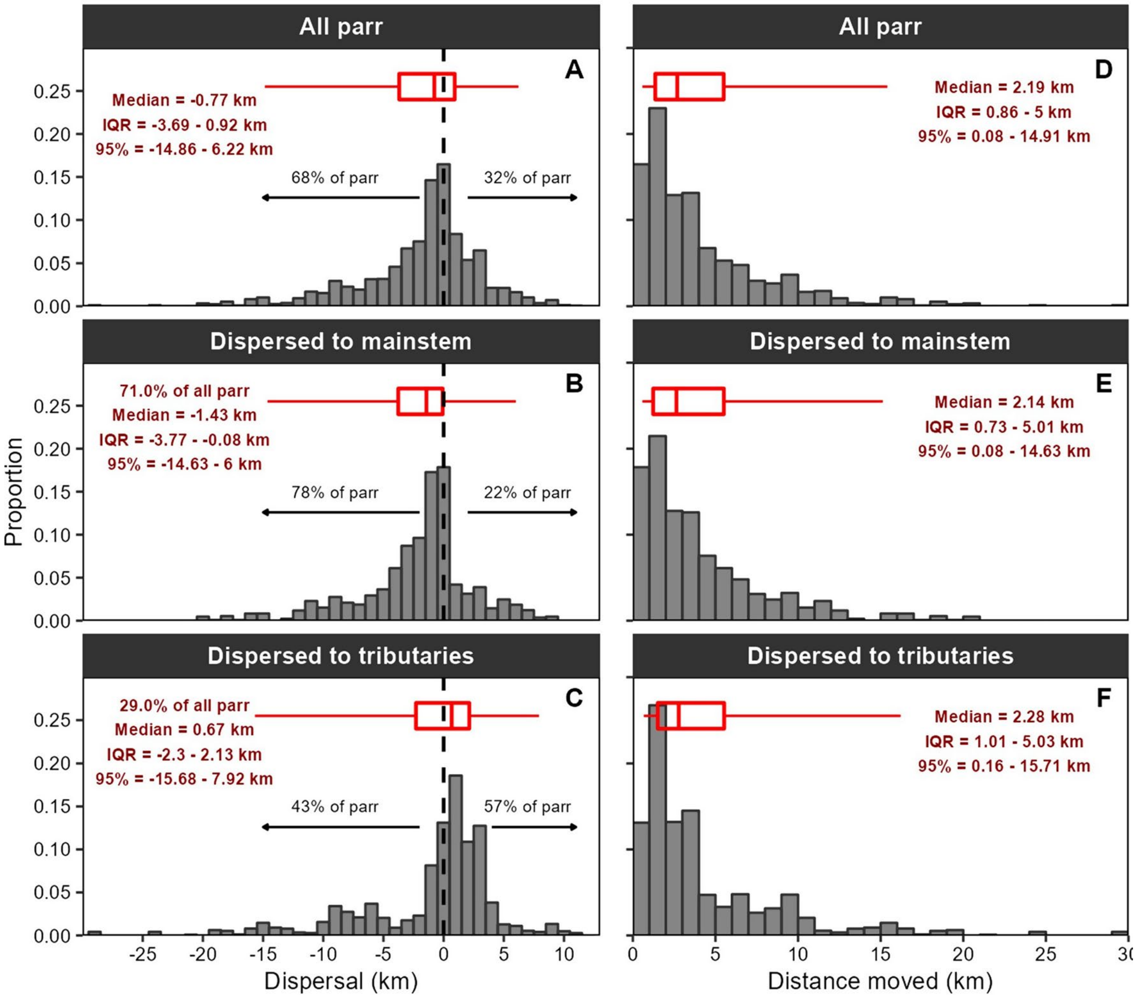

Fig. 3 (**A-C**) Overall distributions of sample-bias corrected dispersal and (**D-F**) total distance moved estimates for (**A**, **D**) all parr (*n* sampled = 1326), (**B**, **E**) parr that dispersed within the mainstem (*n* sampled = 595), and (**C**, **F**) parr that dispersed to tributaries (*n* sampled = 731). Box and whisker plots indicate median, inter-quartile range (IQR), and 95th percentiles

moved (regardless of direction) was 2.2 km and 25% of parr moved farther than 5.0 km (Fig. 3D-F). Parr that dispersed downstream generally moved greater distances (IQR: 0.7–6.0 km; max = 28.6 km) than parr that moved upstream (IQR: 1.1–3.5 km; max = 10.6 km).

Spatial patterns of dispersal

Parr dispersal patterns varied as a function of where they originated (i.e., redd rkm) and dispersed to (i.e., mainstem vs. tributaries; Fig. 4). For parr that dispersed to mainstem locations (Fig. 4A), individuals originating low in the watershed (rkm < 90) exhibited upstream dispersal bias and low variability in dispersal estimates. Dispersal progressively transitioned towards downstream bias for fish originating higher in the watershed, which was accompanied by increasing dispersal variance and range. In contrast, there was little apparent trend between parr origin and dispersal bias or distance

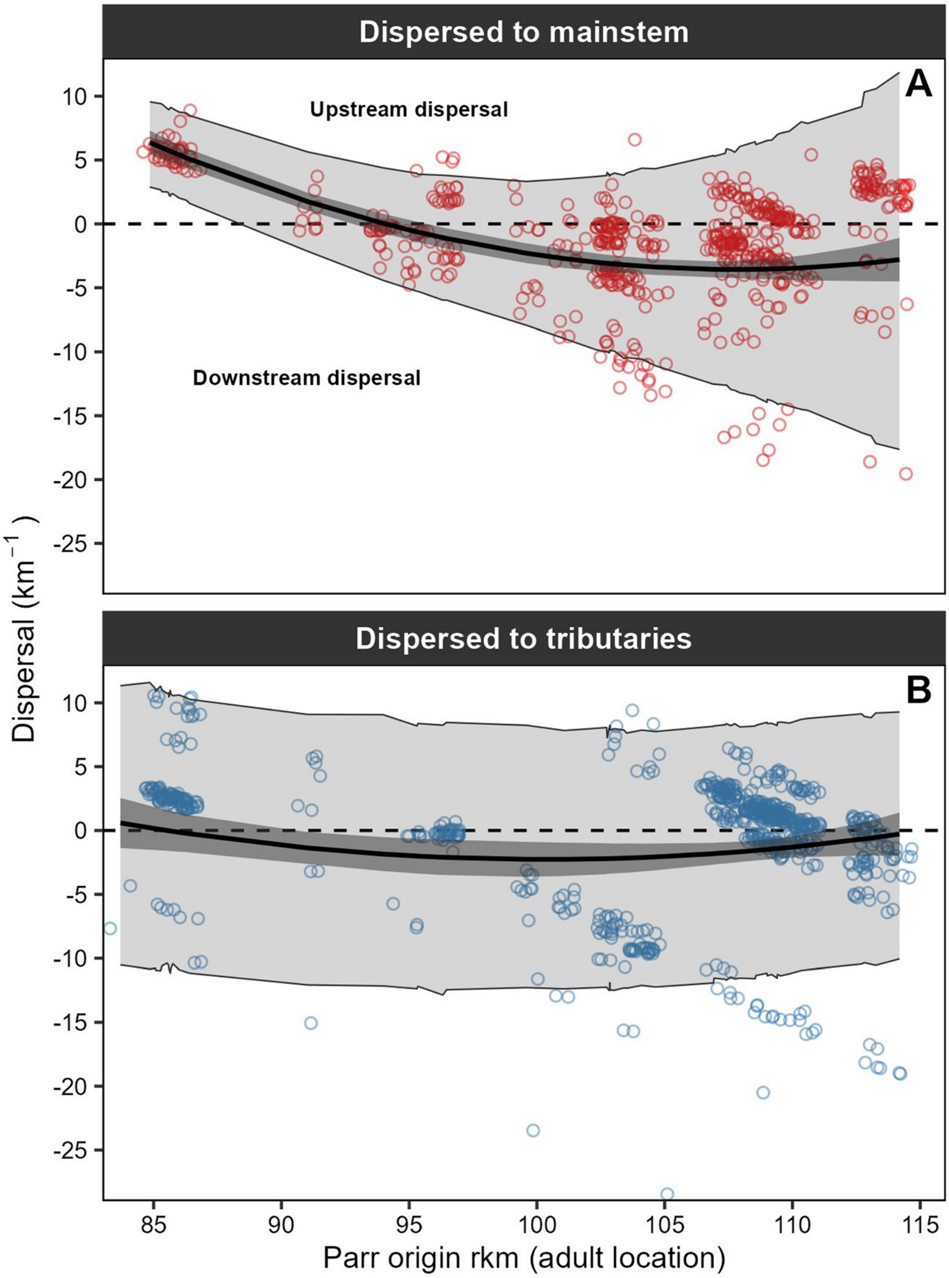

Fig. 4 (**A**) Parr origin (i.e., maternal parent location) versus dispersal for parr captured within the mainstem (red points) and (**B**) within tributaries (blue points). The apparent striation pattern in B is a result of captured parr distributing to, and then relatively small distances (0–1 km) within, spatially-discrete and numerically-fixed tributary confluences ($n = 9$). The solid line indicates the fitted relationship between parr origin and dispersal; dark shading indicates the 95% confidence interval of the fitted relationship; and the light shading indicates the 95% prediction interval

for parr that dispersed to tributaries (Fig. 4B). While it is possible that some parr dispersed downstream beyond our study area, we believe these fish constitute a negligible portion of the population and have minimal effects on overall dispersal patterns at the population-level.

Dispersal patterns generally followed a trend of dispersal from warmer mainstem sections to slightly cooler sections of the mainstem or tributaries (Figs. 5 and 6), which complements patterns between parr distribution and temperature (Fig. 2). For example, parr originating from rkms 84–89, where $\text{MDMT}_{\text{July}}$ exceeded 24.5 °C, either dispersed upstream to cooler mainstem habitats between rkms 91–97 ($\text{MDMT}_{\text{July}} < 23$ °C) or to one of four tributaries between rkms 79.8–96.4 (Fig. 5) where tributary $\text{MDMT}_{\text{July}}$ ranged 17.5–23.1 °C, measured near confluences with the mainstem. This is further exemplified by the inverse relationship between individual parr origin $\text{MDMT}_{\text{July}}$ and the difference between capture and origin $\text{MDMT}_{\text{July}}$ (Fig. 6A; Linear regression, Pearson's $r = -0.46$; $p < 0.001$), and the increasing probability of moving to cooler habitats with warmer parr origin $\text{MDMT}_{\text{July}}$ (Fig. 6B).

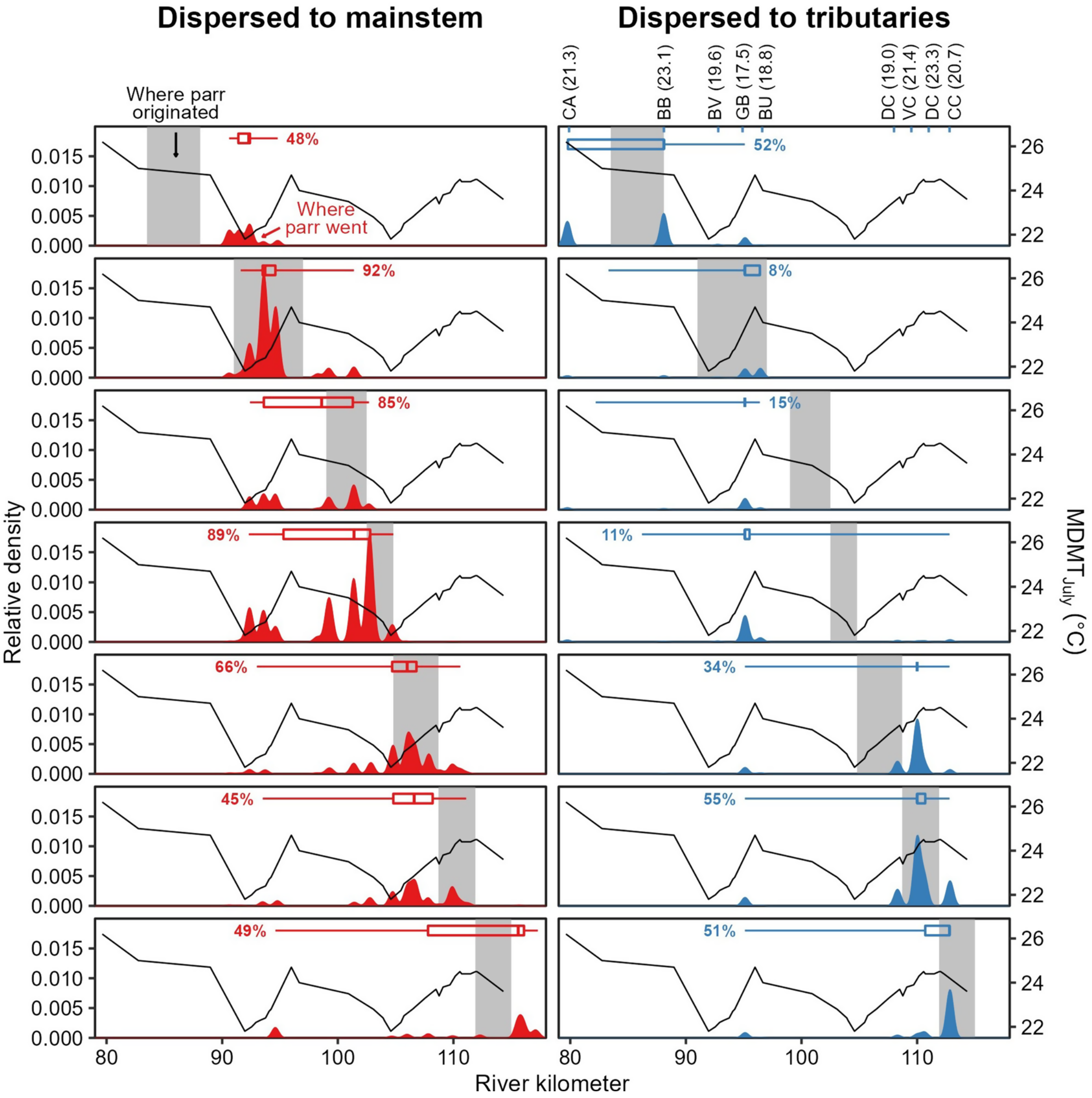

Fig. 5 Parr dispersal patterns from different sections of origin (rows). Grey boxes indicate the section parr originated from; density distributions portray where parr from each section dispersed to across the mainstem (red distributions) and tributaries (blue distributions); box and whisker plots indicate median, inter-quartile range (IQR), and 95th percentiles of parr distributions for each section; percentages indicate the estimated percent of parr from that section that dispersed to mainstem locations (red) or into tributaries (blue); and the solid black line shows maximum temperature ($\text{MDMT}_{\text{July}}$) of the mainstem MFJDR at that location. Tributary $\text{MDMT}_{\text{July}}$ are shown in the right panel in parentheses above tributary abbreviations: CA = Camp Creek, BB = Big Boulder Creek, BV = Beaver Creek, GB = Granite Boulder Creek, BU = Butte Creek, DC = Dead Cow Gulch, VC = Vinegar Creek, DC = Davis Creek, and CC = Clear Creek

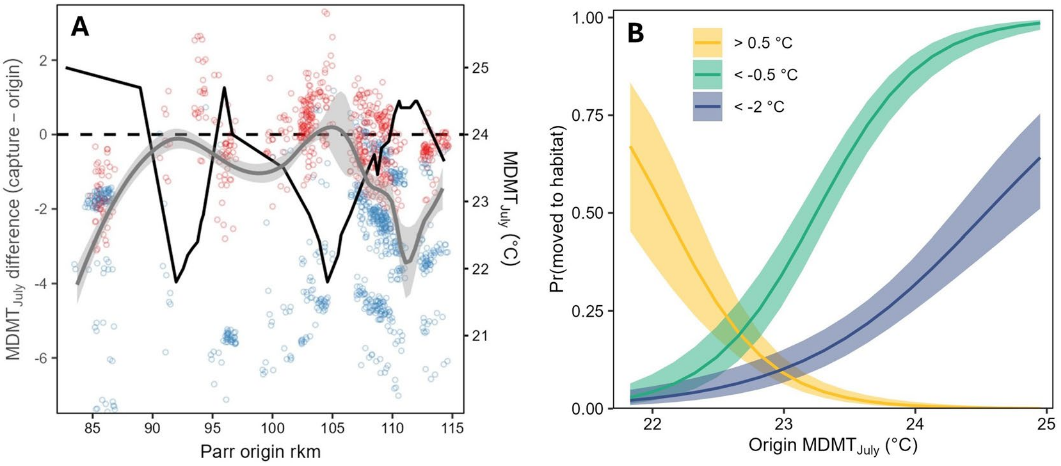

Fig. 6 (**A**) Stream temperature (MDMT$_{July}$; solid black line) and estimated difference in temperature between capture and origin locations for individual parr captured from the mainstem (red points) and tributaries (blue points). The solid grey line in panel A shows a LOESS fit. (**B**) The predicted probability of parr moving to three temperature scenarios – at least 0.5 °C warmer (yellow line), at least 0.5 °C cooler (green line), and at least 2 °C cooler (blue line) – as a function of the temperature (MDMT$_{July}$) at their origin location. The figure highlights that parr originating in warmer areas tended to move to cooler areas

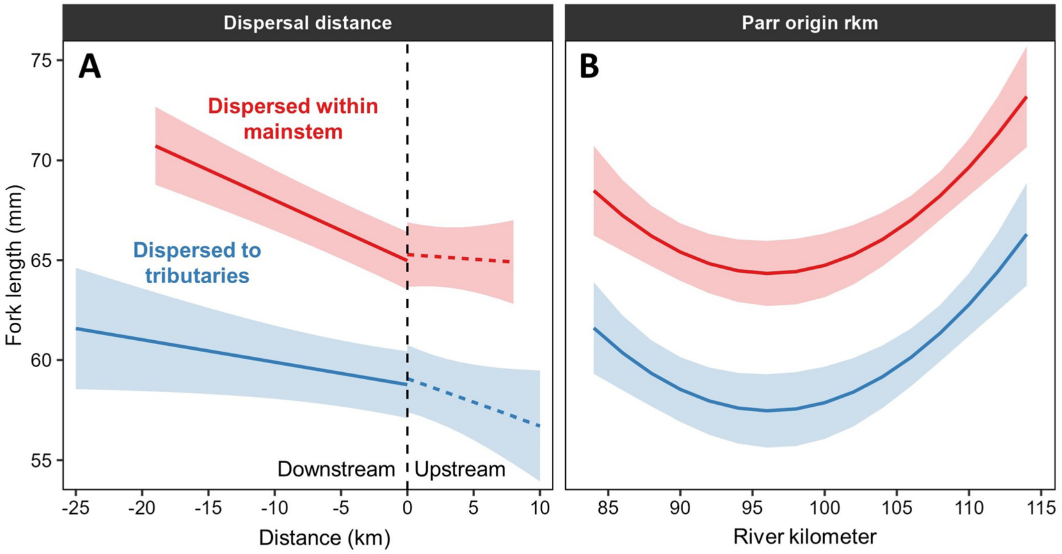

Fig. 7 Marginal effects of (**A**) dispersal distance and (**B**) parr origin river kilometer on post-dispersal parr fork length (e.g., length-at-capture) after accounting for effects of date of sampling, capture location temperature and capture location density (see Additional file 1: Fig. S8 for covariate effects). Model selection indicated that the relationship between dispersal distance and fork length was dependent on whether parr dispersed within the mainstem (red) or to tributaries (blue) and whether parr dispersed downstream (solid lines) or upstream (dashed lines). Longitudinal patterns of parr fork length (**B**) are inversely related to estimated emergence timing, which was progressively earlier upstream of rkm 100 (Additional file 1: Fig. S2)

Longitudinal patterns in parr distribution varied considerably as a function of where juveniles originated (Fig. 5). For example, rkms 91–97 supported parr originating from nearly all parts of the watershed, whereas sections upstream only supported parr originating from nearby. Similarly, some tributaries such as Granite Boulder (rkm 95.1) supported parr originating across a wide spatial extent, whereas upstream tributaries supported parr from within several kilometers.

Post-dispersal size

The best model predicting parr length-at-capture across the MFJDR indicated that the effect of dispersal distance was dependent on dispersal direction (upstream vs. downstream) and capture location (mainstem vs. tributaries; Fig. 7A; Additional File 1: Table S1). Dispersal distance was associated with longer length-at-capture for parr that dispersed downstream, and the effect was greater for parr that dispersed within the mainstem (0.30 mm km^{-1}; 95% CI: 0.22–0.39; $p < 0.001$) versus into tributaries (0.11 mm km^{-1}; 95% CI: 0.00–0.23;

$p = 0.056$). In contrast, there was little trend between upstream dispersal distance and post-dispersal length for parr that dispersed within the mainstem (-0.04 mm km^{-1}; 95% CI = -0.31–0.21; $p = 0.727$), but there was a negative relationship associated with dispersal to tributaries (-0.24 mm km^{-1}; 95% CI = -0.50–0.03; $p = 0.077$). Independent of dispersal, parr were predicted to average 6.2 mm longer when captured in the mainstem versus tributaries (95% CI = 4.97–7.75; $p < 0.001$), but that the additive effect of upstream versus downstream dispersal was minimal (95% CI = -0.59–1.20 mm; $p = 0.304$). Parr length-at-capture was also spatially structured (Fig. 7B), exhibiting a parabolic pattern with nearly a 10 mm difference between parr originating farthest upstream (rkm 114) compared to middle sections (rkms 90–100) where predicted lengths were shortest. Later sampling dates (0.09 mm day^{-1}; 95% CI = 0.06–0.12; $p < 0.001$) and higher parr densities (0.22 mm parr m^{-1}; 95% CI = 0.06–0.38; $p = 0.007$) were associated with longer length-at-capture, whereas warmer maximum temperatures (MDMT$_{\text{July}}$) were associated with decreasing length (-1.09 mm °C; 95% CI = -1.38– -0.80; $p < 0.001$; Additional File 1: Fig. S7). Collectively, the model fixed-effects explained 38% of the variation in length-at-capture and 65% with the random effect of unique female parent.

Discussion

We used genetic PBT to directly quantify wild juvenile Chinook Salmon dispersal from their origin to summer rearing habitats throughout the MFJDR riverscape. Fish dispersed considerable distances (median = 2.2 km, max = 28.6 km), moving not only up or down the mainstem, but also into tributaries. We documented more extensive dispersal compared to prior studies conducted at smaller spatial scales or in experimental settings (see review by Eisenhauer et al. [27]). This suggests dispersal in wild populations may be higher in magnitude than currently recognized [11–13], and (by extension) that the spatial configuration of spawning and rearing habitat is less constraining than previously thought. We found clear patterns in dispersal explained by initial landscape position and water temperature. Fish originating upstream tended to move downstream and vice versa. Nested within that broader pattern, fish responded to reach-level thermal heterogeneity, such that if they originated in reaches that became among the warmest during summer, they tended to disperse to cooler mainstem reaches or tributaries. This is a novel example of adaptive capacity [48] analogous to salmonids that spawn in ephemeral streams and disperse to perennial mainstems [49]. Lastly, our results suggest that broad patterns in biophysical processes across the riverscape – spatial structuring of emergence timing in this case – may shape the competitive advantages of dispersal strategies. In the MFJDR, emergence timing is progressively earlier upstream due to contributions of warmer groundwater in winter [29]. Individuals that disperse downstream should have competitive advantages (i.e., size and dominance hierarchies) over later emerging conspecifics, whereas upstream dispersal should be competitively disadvantageous, which was supported by a positive effect of dispersal distance on parr length-at-capture for downstream dispersal but not for upstream dispersal. Collectively, this study provides an approach to effectively evaluate riverscape patterns and drivers of juvenile salmonid dispersal in naturally spawning populations that can be applied to other river systems, species, and life-stages.

Thermal conditions

Chinook parr dispersed from warmer sections of the river to cooler mainstem sections or into tributaries (e.g., Figs. 5 and 6). Fish originating from areas in the MFJDR where MDMT$_{\text{July}}$ exceeded 23 °C were captured as parr in areas that averaged 2.5 °C cooler, suggesting temperature is one of the dominant mechanisms driving dispersal. We found the highest densities of Chinook parr in the MFJDR where cool-water tributaries likely contributed to lower mainstem temperatures, or within those cool-water tributaries, as not all tributaries offered thermal refugia (Table 1). Previous studies have found that tributaries and their confluences often provide thermal refuges for salmonids [50–52] as tributaries often have greater groundwater inputs and shade [53] compared to mainstem river channels. These thermal refuges allow salmonids to endure in river systems where many areas become thermally unsuitable during summer months [52]. Our parr sampling in the summer of 2021 occurred as the Pacific Northwest experienced a record-breaking heat dome [54], possibly amplifying dispersal behavior from warmer to cooler habitats within the MFJDR and into tributaries. The climate conditions experienced in 2021 are predicted to increase in frequency and intensity [54, 55], and dispersal may become increasingly necessary for warmer sections of this watershed and others to remain productive spawning and early rearing habitats. Yet, if thermal refuges are limited, density-dependent factors could limit growth and survival in these areas [28].

Dispersal extent and context

Despite extensive research on fish spatial ecology, a knowledge gap exists for early life histories because these individuals are typically too small to track using conventional tagging approaches (e.g., telemetry tags, PIT tags). By applying genetic parentage analysis to parr sampled across the spawning and rearing extent, our study provides an assessment of the full range of dispersal patterns expressed by a wild population of juvenile Chinook Salmon. Our results suggest that collectively, the widespread dispersal upstream, downstream, and into tributaries generated a continuum of overall mobility during this nonmigratory period. There was no evidence supporting the binary concept of "movers" and "stayers" [13], characterized by a bimodal distribution of mobile and stationary individuals; however, the expression of distinct mobile and stationary groups may occur in other populations and at later life stages due to differences in genetic predisposition, environmental conditions, and biological factors. The dispersal distances and patterns observed in this study could be viewed as a challenge to the Restricted Movement Paradigm [48], or alternatively, as an extension. In a review of published estimates of juvenile Atlantic salmon dispersal, Eisenhauer et al. [24] found that dispersal was generally downstream-biased and that nearly all individuals dispersed less than 0.5 km; however, the authors also presented original empirical results from 19 tributaries, in which a third of fish moved upstream and dispersal distances were more variable, with higher maximums (~ 3 km upstream and ~ 5 km downstream). Our results similarly suggest that approximately a third of individuals dispersed upstream, but that maximum dispersal distance was even greater (~ 28 km downstream and ~ 11 km upstream). Yet the distribution of dispersal distances was centered near zero (median = 0.77 km downstream; Fig. 3A), and most individuals moved short distances relative to all distances observed, which conforms with the RMP, but suggests the need for flexibility in how we define "restricted movement" across watersheds, populations, and species.

Longitudinal dispersal patterns

Parr originating higher in the watershed exhibited greater variability in dispersal than parr originating lower in the basin. Prior studies suggest that high variation in dispersal patterns are characteristic responses to variability in biophysical conditions and behavioral selection specific to localized watershed characteristics. For example, previous research has demonstrated extensive dispersal patterns of recently emerged salmon fry (10–100 s of kilometers) associated with alternative early life-history strategies [24, 30, 56, 57]. Within the MFJDR, variable dispersal may be attributed to several potential factors. First, progressively earlier emergence timing with distance upstream translated to fry being exposed to high flows for longer durations in this snowmelt-dominated system (Additional File 1: Fig. S1), which by extension, could result in greater passive downstream dispersal. Alternatively, the longer duration since emergence and larger size of parr upstream suggests that differences in ontogeny could have been a contributing factor to greater dispersal variability. Larger individuals often disperse farther than smaller conspecifics [15, 23] and variability in dispersal may increase in later life stages [58] as density-dependence exerts greater influence on dispersal [28]. A portion of longitudinal dispersal patterns could also be attributed to genetic effects stemming from fine-scale selection on dispersal strategies [59] from specific locations within the watershed to optimize survival over long time periods. Lastly, these patterns could also be attributed to the directional flow of river networks interacting with environmental conditions that contracted the juvenile rearing distribution. High summer temperatures were clearly a factor influencing dispersal and ultimately parr distribution. However, parr from upstream locations could move downstream with the flow to cooler habitats (e.g., tributary junctions), whereas parr originating downstream needed to move upstream against the current to find more thermally suitable habitat, thereby incurring higher energetic costs of movement. Thus, dispersal was constrained by the extent of suitable rearing habitat, such that most available suitable habitat was downstream for upstream-originating fish, whereas downstream-originating fish experienced the opposite. This phenomenon of fish being "hemmed in" by thermal boundaries should theoretically occur when unfavorable offspring rearing conditions contract the extent of suitable rearing habitats from the initial spawning extent, whereas the opposite effect may manifest when adult spawners experience less favorable conditions than their offspring, causing expansion of the rearing extent. Across riverscapes, the conditions experienced across the parent-offspring life stages may be an important factor driving inter-annual variability in dispersal patterns.

Dispersal patterns and post-dispersal size

After accounting for parr origin rkm (and by extension emergence timing) and other factors expected to influence parr body size, dispersal distance was associated with longer length-at-capture for parr that dispersed downstream, but not upstream. Mid-summer size integrates growth prior to, during, and after dispersal; consequently, the degree to which these findings reflect effects of size-at-dispersal vs. post-dispersal growth is uncertain, but our data provide insights to evaluate several potential mechanisms. Most studies report positive relationships between both downstream and upstream dispersal distance and size-at-dispersal [15, 23, 27, 60], which could result from greater swimming capacity of larger individuals or if farther dispersal is associated with more favorable growth conditions (e.g., lower densities, higher prey availability) increasing post-dispersal growth [22]. It is unlikely that greater swimming capacity of larger individuals would result in farther dispersal distances downstream but not upstream. Model selection indicated a positive effect of parr density on post-dispersal size, which opposes the expected negative effect associated with density-dependence. We propose that there was a competitive advantage for individuals dispersing downstream but not upstream, stemming from the longitudinal structuring of emergence timing in the MFJDR (progressively earlier upstream). Early emergence provides competitive advantages over later-emerging conspecifics including larger size and the establishment of dominant feeding positions through prior residency [61]. Downstream dispersal should afford competitive advantages over later emerging conspecifics, and the advantage should increase with distance downstream. In contrast, it would be challenging for individuals that disperse upstream to establish a competitive advantage since habitat occupancy and feeding positions are more likely to be established by conspecifics that are larger on average. In other river systems in which emergence timing occurs progressively later upstream [29], we hypothesize that competitive advantages would flip, favoring upstream dispersal.

Study considerations

Correcting for sampling bias had considerable effects on interpretation of dispersal patterns in the MFJDR (Additional File 1: Fig. S8). For example, dispersal was not biased upstream or downstream using uncorrected dispersal estimates (median = -0.03 km; 50% dispersed in each direction), but when sampling-bias corrections were applied, the overall dispersal distribution was clearly downstream-biased (median = -0.77 km; 68% dispersed downstream). This highlights the importance of obtaining a random sample of the population [42], or correcting for any sample biases, when quantifying dispersal. While it is ideal to minimize sampling bias through careful study design, if possible, we believe our approach effectively reduced sampling bias and improved characterization of population-level dispersal. If characterizing parr distribution is not a study objective, an alternative approach with fewer logistical challenges would be to conduct equal-effort sampling and genotyping all (or a consistent proportion) of the juveniles captured at randomly selected habitats across the rearing extent.

There are a number of considerations associated with our study design and characterizing dispersal patterns for wild fish populations. First, we did not sample parr or conduct abundance surveys in the mainstem or tributaries downstream of Camp Creek and we were not able to sample all tributaries continuously. Consequently, our results may not reflect the full extent of dispersal and distribution present within this population. However, few age-0 juveniles from the MFJDR are captured in a downstream screw trap and downstream rearing is not thought to be a common life history (Ian Tattam; unpublished data). Thus, we hypothesize that parr dispersal outside of our study area likely had minimal effects on overall dispersal patterns at the population-level. Second, it is important to note that our dispersal estimates only represent individuals that survived to summer and that our approach defines dispersal based on two points in time. Sampling earlier in the year may have revealed different patterns, such as greater downstream bias associated with passive dispersal of recently emerged fry exposed to high flows [62]. It is likely that some individuals passively dispersed downstream and later moved upstream [58], but our sampling approach would not detect these patterns. Third, we were only able to sample a portion of the adult spawning population and the number of parr assigned to each female was not uniform with approximately 25% of females accounting for 50% of parr-female assignments. Thus, dispersal estimates only represent juveniles from a subset of female spawners, and although we included random effects for female parent in models, results may be further influenced by relatedness that we were unable to account for (e.g., paternal relatedness). Lastly, the early summer of 2021 was characterized by abnormally high air and water temperatures and low discharge. The dispersal patterns we observed, especially the effect of summer temperature on dispersal and parr distribution, likely differ considerably in cooler years with greater summer baseflow. On the other hand, the conditions were representative of those anticipated under climate change and our results provide insight into fish movement responses and the habitat attributes and locations that are likely to become increasingly important.

Conclusions

In a dendritic watershed, the majority of spring Chinook Salmon parr that survived to mid-summer (73%) occupied habitats within the mainstem river where nearly all spawning had occurred. Dispersal was widespread within the mainstem and into the tributaries, occurring in both downstream and upstream directions. Our results suggest that immigration into tributaries was driven primarily by behavioral thermoregulation. While tributaries to the MFJDR function as important summer thermal refuge, aggregation of parr in the tributaries could have density-dependent effects on growth and survival. Cooler sections of the mainstem – much of which have been the target of extensive restoration – supported the highest parr abundances, and downstream sections hosted parr originating from the broadest range of spawning locations whereas parr inhabiting upstream sections originated from a narrower spatial extent. This suggests that restoration of thermally tolerable habitat in these lower mainstem reaches will benefit parr from throughout the watershed and may be critical to maintain downstream sections as productive spawning habitats. Collectively, these observations suggest that improvement and downstream expansion of suitable rearing habitat in the mainstem of the MFJDR and similar rivers in the interior

Columbia River Basin will be required to reach biological and sociological recovery thresholds.

Abbreviations

km	Kilometers
RMP	Restricted Movement Paradigm
PBT	Parentage-based tagging
MFJDR	Middle Fork John Day River
RKMS	River kilometers
CFS	Cubic feet per second
ODFW	Oregon Department of Fish and Wildlife
CTWSRO	Confederated Tribes of the Warm Springs Reservation of Oregon
GPS	Global positioning system
m	Meters
mm	Millimeters
km	Kilometer
g	Grams
DNA	Deoxyribonucleic acid
SNPs	Single nucleotide polymorphisms
LLR	Log-likelihood ratio
FNT	Fast-non-turbulent
FT	Fast-turbulent
QAQC	Quality assurance/quality control
MDMT	Mean daily maximum temperature
IQR	Inter-quartile range
GLMM	General linear mixed-effects model
CI	Confidence interval
°C	Degree Celsius

Supplementary Information

The online version contains supplementary material available at https://doi.org/10.1186/s40462-024-00524-3.

Supplementary Material 1

Acknowledgements
Implementing this study would not have been possible without the contributions of numerous agencies and individuals who aided in field efforts, planning, providing data, and interpreting results. Spawning surveys were conducted by ODFW, CTWSRO, the North Fork and South Fork John Day Watershed Councils, the U.S. Forest Service, and volunteers from numerous other agencies. We especially thank C. Bare for efforts to coordinate spawning surveys and modify protocols to accommodate this study. We thank the numerous individuals who assisted in juvenile fish sampling including, but not limited to J. Bailey, E. Blackburn, E. Booher, M. Cottingham, Z. Cunningham, H. Latzo, T. Sparrow, L. Osborne, C. Sheen, and A. Woolen. Temperature data were maintained and provided by the Middle Fork John Day Intensively Monitored Watershed's (MFIMW) Water Temperature Monitoring Subgroup. Additional logistical and planning support was provided by the MFIMW, particularly E. Booher and K. Bliesner. Genotyping was supported in the laboratory by E. Collins, L. Maxwell, and M. Moore and E. Collins supported genotyping analyses. We also thank two anonymous reviewers for constructive feedback on the manuscript. J. Hetfield, L. Ulrich, K. Hammett, R. Trujillo, and J. Newsted provided instrumental motivation and creative inspiration during manuscript preparation.

Author contributions
JL and MK conceptualized the study with input from SW. JL, LC, MF, MK, and SW designed the study with input from BS, CJ, IT, SK, and SN. JL, LC, MF, MK, and SK led data collection with the help of numerous others. MK led data analysis with contributions from BS, CJ, LC, MF, JA, JL, and SW. MK drafted the original version of the manuscript with contributions from JL, LC and MF. BS, CJ, IT, JA, JL, LC, MF, SN and SW revised the manuscript and all authors reviewed and approved the final draft.

Funding
This research was supported by Bonneville Power Administration (BPA) funds as part of the Columbia Basin Fish Accords Agreement (project numbers 2009-004-00 & 2007-397-00), BPA funds administered to ODFW (project 1998-016-00), Pacific States Marine Fisheries Commission funds administered by the Oregon Watershed Enhancement Board, State of Oregon General funds, and the Bureau of Reclamation (adult salmon genotyping costs).

Data availability
All data used in the analyses contained in this article are stored in an archived GitHub repository (https://doi.org/10.5281/zenodo.14549890).

Declarations

Ethics approval and consent to participate
Fish sampling and handling protocols were approved by the Oregon State University Animal Care and Use Committee (IACUC-2019-0006).

Consent for publication
Not applicable.

Competing interests
The authors declare no competing interests.

Author details
[1]Fishery Science Department, Columbia River Inter-Tribal Fish Commission, Portland, OR 97232, USA
[2]Oregon Department of Fish and Wildlife, East Region Fish Research, La Grande, OR 97850, USA
[3]Department of Fisheries, Wildlife, and Conservation Sciences, Oregon State University, Corvallis, OR 97330, USA
[4]Confederated Tribes of the Warm Springs Reservation of Oregon, John Day, OR 97845, USA
[5]Hagerman Genetics Lab, Columbia River Inter-Tribal Fish Commission, Hagerman, ID 83332, USA

Received: 22 April 2024 / Accepted: 13 December 2024

References
1. Stanford JA, Lorang MS, Hauer FR. The shifting habitat mosaic of river ecosystems. SIL Proceedings, 1922–2010. 2005;29:123–36.
2. Griffen BD, Norelli AP. Spatially variable habitat quality contributes to within-population variation in reproductive success. Ecol Evol. 2015;5:1474–83.
3. Turlure C, Schtickzelle N, Dubois Q, Baguette M, Dennis RLH, Van Dyck H. Suitability and transferability of the resource-based habitat concept: a test with an assemblage of butterflies. Front Ecol Evol. 2019;7:127.
4. Einum S, Nislow KH, Mckelvey S, Armstrong JD. Nest distribution shaping within-stream variation in Atlantic salmon juvenile abundance and competition over small spatial scales. J Anim Ecol. 2008;77:167–72.
5. Yoshimoto J. Interspecific variation in competitor avoidance and foraging success in sap-attracted insects. Eur J Entomol. 2009;106:529–33.
6. Hahlbeck N, Tinniswood WR, Sloat MR, Ortega JD, Wyatt MA, Hereford ME et al. Contribution of warm habitat to cold-water fisheries. Conservation Biology [Internet]. 2022 [cited 2023 May 22];36. https://onlinelibrary.wiley.com/doi/https://doi.org/10.1111/cobi.13857
7. Elmore RD, Carroll JM, Tanner EP, Hovick TJ, Grisham BA, Fuhlendorf SD, et al. Implications of the thermal environment for terrestrial wildlife management. Wildl Soc Bull. 2017;41:183–93.
8. Armstrong JB, Schindler DE, Omori KL, Ruff CP, Quinn TP. Thermal heterogeneity mediates the effects of pulsed subsidies across a landscape. Ecology. 2010;91:1445–54.
9. Baldock JR, Armstrong JB, Schindler DE, Carter JL. Juvenile coho salmon track a seasonally shifting thermal mosaic across a river floodplain. Freshw Biol. 2016;61:1454–65.
10. Aikens EO, Kauffman MJ, Merkle JA, Dwinnell SPH, Fralick GL, Monteith KL. The greenscape shapes surfing of resource waves in a large migratory herbivore. Nathan R, editor. Ecol Lett. 2017;20:741–50.
11. Gerking SD. The restricted movement of fish populations. Biol Rev. 1959;34:221–42.
12. Gowan C, Young MK, Fausch KD, Riley SC. Restricted movement in resident stream salmonids: a paradigm lost? Can J Fish Aquat Sci. 1994;51:2626–37.

13. Rodriguez MA. Restricted movement in stream fish: the paradigm is incomplete, not lost. Ecology. 2002;83:1–13.
14. Morrissey MB, Ferguson MM. Individual variation in movement throughout the life cycle of a stream-dwelling salmonid fish. Mol Ecol. 2011;20:235–48.
15. Anderson JH, Pess GR, Kiffney PM, Bennett TR, Faulds PL, Atlas WI, et al. Dispersal and tributary immigration by juvenile coho salmon contribute to spatial expansion during colonisation. Ecol Freshw Fish. 2013;22:30–42.
16. Hudy M, Coombs JA, Nislow KH, Letcher BH. Dispersal and within-stream spatial population structure of Brook Trout revealed by pedigree reconstruction analysis. Trans Am Fish Soc. 2010;139:1276–87.
17. Einum S, Nislow KH. Local-scale density-dependent survival of mobile organisms in continuous habitats: an experimental test using Atlantic salmon. Oecologia. 2005;143:203–10.
18. Teichert MAK, Foldvik A, Forseth T, Ugedal O, Einum S, Finstad AG et al. Effects of spawning distribution on juvenile Atlantic salmon (*Salmo salar*) density and growth. Grant J, editor. Can J Fish Aquat Sci. 2011;68:43–50.
19. Einum S, Robertsen G, Nislow KH, McKelvey S, Armstrong JD. The spatial scale of density-dependent growth and implications for dispersal from nests in juvenile Atlantic salmon. Oecologia. 2011;165:959–69.
20. Beechie T, Moir H, Pess G. Hierarchical physical controls on salmonid spawning location and timing. Am Fish Soc Symp. 2008;65:83–101.
21. Flitcroft R, Burnett K, Snyder J, Reeves G, Ganio L. Riverscape patterns among years of juvenile coho salmon in midcoastal Oregon: implications for conservation. Trans Am Fish Soc. 2014;143:26–38.
22. Brunsdon EB, Fraser DJ, Ardren WR, Grant JWA. Dispersal and density-dependent growth of Atlantic salmon (*Salmo salar*) juveniles: clumped versus dispersed stocking. Can J Fish Aquat Sci. 2017;74:1337–47.
23. Aparicio E, Rocaspana R, De Sostoa A, Palau-Ibars A, Alcaraz C. Movements and dispersal of brown trout (*Salmo trutta* Linnaeus, 1758) in Mediterranean streams: influence of habitat and biotic factors. PeerJ. 2018;6:e5730.
24. Scheu MP. Downstream rearing Chinook Salmon (*Oncorhynchus tshawytscha*) in the Upper Mainstem of the John Day River [Internet] [Masters]. [Corvallis, Oregon]: Oregon State University; 2022. https://ir.library.oregonstate.edu/concern/graduate_thesis_or_dissertations/b2774406b
25. Foldvik A, Finstad AG, Einum S. Relating juvenile spatial distribution to breeding patterns in anadromous salmonid populations. J Anim Ecol. 2010;79:501–9.
26. Atlas WI, Buehrens TW, McCubbing DJF, Bison R, Moore JW. Implications of spatial contraction for density dependence and conservation in a depressed population of anadromous fish. Can J Fish Aquat Sci. 2015;72:1682–93.
27. Eisenhauer ZJ, Christman PM, Matte J-M, Ardren WR, Fraser DJ, Grant JWA. Revisiting the restricted movement paradigm: the dispersal of Atlantic salmon fry from artificial redds. Can J Fish Aquat Sci. 2021;78:493–503.
28. Einum S, Sundt-Hansen L, Nislow H. The partitioning of density-dependent dispersal, growth and survival throughout ontogeny in a highly fecund organism. Oikos. 2006;113:489–96.
29. Kaylor MJ, Armstrong JB, Lemanski JT, Justice C, White SM. Riverscape heterogeneity in estimated Chinook Salmon emergence phenology and implications for size and growth. Ecosphere [Internet]. 2022 [cited 2023 May 19];13. https://onlinelibrary.wiley.com/doi/https://doi.org/10.1002/ecs2.4160
30. Bradford MJ, Taylor GC. Individual variation in dispersal behaviour of newly emerged chinook salmon (*Oncorhynchus tshawytscha*) from the Upper Fraser River, British Columbia. Can J Fish Aquat Sci. 1997;54:1585–92.
31. Bare CM, Tattam IA, Ruzycki JR. Chinook Salmon productivity and escapement monitoring in the John Day River basin [Internet]. John Day, OR: Oregon Department of Fish and Wildlife; 2021. http://www.middleforkimw.org/uploads/6/7/8/9/67899115/jd_chs_sy2018_adult_annual.pdf
32. Copeland T, Venditti DA. Contribution of three life history types to smolt production in a Chinook salmon (*Oncorhynchus tshawytscha*) population. Jonsson B, editor. Can J Fish Aquat Sci. 2009;66:1658–65.
33. Torgersen CE, Baxter CV, Li HW, McIntosh BA. Landscape influences on longitudinal patterns of river fishes: Spatially continuous analysis of fish-habitat relationships. American Fisheries Society Symposium. 2006;48:473–92.
34. Stevens DL, Olsen AR. Spatially balanced sampling of natural resources. J Am Stat Assoc. 2004;99:262–78.
35. Campbell NR, Harmon SA, Narum SR. Genotyping-in-thousands by sequencing (GT-seq): a cost effective SNP genotyping method based on custom amplicon sequencing. Mol Ecol Resour. 2015;15:855–67.
36. Hess JE, Horn RL, Stephenson J, Willis S, Narum SR. Genetic assessment of Columbia River Stocks, 1/1/2022–12/31/2022 Annual Report, 2008-907-00 [Internet]. Portland, OR: Columbia River Inter-Tribal Fish Commission; 2023 p. 405. Report No.: Technical Report 23 – 02. https://critfc.org/reports/2022-annual-report-genetic-assessment-of-columbia-river-stocks/
37. Anderson EC, CKMRsim. Inference of pairwise relationships using likelihood ratios. R package version 0.1.2.999. 2020.
38. Bravington MV, Skaug HJ, Anderson EC. Close-Kin Mark-Recapture. Statist Sci [Internet]. 2016 [cited 2023 May 19];31. https://projecteuclid.org/journals/statistical-science/volume-31/issue-2/Close-Kin-https://doi.org/10.1214/16-STS552.full
39. Murdoch AR, Pearsons TN, Maitland TW. Use of carcass recovery data in evaluating the spawning distribution and timing of spring Chinook Salmon in the Chiwawa River, Washington. North Am J Fish Manag. 2009;29:1206–13.
40. Kaylor MJ, Justice C, Armstrong JB, Staton BA, Burns LA, Sedell E, et al. Temperature, emergence phenology and consumption drive seasonal shifts in fish growth and production across riverscapes. J Anim Ecol. 2021;90:1727–41.
41. Staton BA, Justice C, White S, Sedell ER, Burns LA, Kaylor MJ. Accounting for uncertainty when estimating drivers of imperfect detection: an integrated approach illustrated with snorkel surveys for riverine fishes. Fish Res. 2022;249:106209.
42. Wacker S, Skaug HJ, Forseth T, Solem Ø, Ulvan EM, Fiske P, et al. Considering sampling bias in close-kin mark–recapture abundance estimates of Atlantic salmon. Ecol Evol. 2021;11:3917–32.
43. Feden MJ, Bliesner KL. Water temperature monitoring strategy for the Middle Fork John Day intensively monitored watershed 2022–2023. John Day, Oregon: Middle Fork John Day Water Temperature Monitoring Subgroup; 2022.
44. Burnham KP, Anderson DR. Multimodel inference: understanding AIC and BIC in model selection. Sociol Methods Res. 2004;33:261–304.
45. Brooks ME, Kristensen K, van Benthem KJ, Magnusson A, Berg CW, Nielsen A, et al. glmmTMB balances speed and flexibility among packages for zero-inflated generalized linear mixed modeling. R J. 2017;9:378–400.
46. Hartig F, DHARMa. Residual Diagnostics for Hierarchical (Multi-Level / Mixed) Regression Models [Internet]. 2022. https://CRAN.R-project.org/package=DHARMa
47. Dormann CF, Elith J, Bacher S, Buchmann C, Carl G, Carré G, et al. Collinearity: a review of methods to deal with it and a simulation study evaluating their performance. Ecography. 2013;36:27–46.
48. Beever EA, O'Leary J, Mengelt C, West JM, Julius S, Green N, et al. Improving conservation outcomes with a new paradigm for understanding species' fundamental and realized adaptive capacity. Conserv Lett. 2016;9:131–7.
49. Everest FH. Ecology and management of summer steelhead in the Rogue River - Fishery Research Report Number 7. Corvallis, OR: Oregon State Game Commission; 1973. p. 45.
50. Sutton RJ, Deas ML, Tanaka SK, Soto T, Corum RA. Salmonid observations at a Klamath River thermal refuge under various hydrological and meteorological conditions. River Res Apps. 2007;23:775–85.
51. Brewitt KS, Danner EM. Spatio-temporal temperature variation influences juvenile steelhead (*Oncorhynchus mykiss*) use of thermal refuges. Ecosphere. 2014;5:1–26.
52. Wang T, Kelson SJ, Greer G, Thompson SE, Carlson SM. Tributary confluences are dynamic thermal refuges for a juvenile salmonid in a warming river network. River Res Apps. 2020;36:1076–86.
53. Dralle DN, Hahm WJ, Rempe DM, Karst NJ, Thompson SE, Dietrich WE. Quantification of the seasonal hillslope water storage that does not drive streamflow. Hydrol Process. 2018;32:1978–92.
54. White RH, Anderson S, Booth JF, Braich G, Draeger C, Fei C, et al. The unprecedented Pacific Northwest heatwave of June 2021. Nat Commun. 2023;14:727.
55. Fischer EM. Increasing probability of record-shattering climate extremes. Nat Clim Change. 2021;11.
56. Daum DW, Flannery BG. Canadian-origin Chinook Salmon rearing in non-natal U.S. tributary streams of the Yukon Tiver. Alaska Trans Am Fisheries Soc. 2011;140:207–20.
57. Schroeder RK, Whitman LD, Cannon B, Olmsted P. M Rennie editor 2016 Juvenile life-history diversity and population stability of spring Chinook salmon in the Willamette River basin, Oregon. Can J Fish Aquat Sci 73 921–34.
58. Yamamoto T, Kitanishi S, Metcalfe NB. Effect of parental phenotype on dispersal, growth and maturation of offspring in wild masu salmon (*Oncorhynchus masou*). Evol Ecol. 2021;35:253–69.
59. Kanno Y, Vokoun JC, Letcher BH. Fine-scale population structure and riverscape genetics of brook trout (Salvelinus fontinalis) distributed continuously along headwater channel networks. Mol Ecol. 2011;20:3711–29.

60. Close TL, Anderson CS. Dispersal, density-dependent growth, and survival of stocked steelhead fry in Lake Superior tributaries. North Am J Fish Manag. 1992;12:728–35.
61. Einum S, Fleming IA. Selection against late emergence and small offspring in Atlantic salmon (*Salmo salar*). Evolution. 2000;54:628–39.
62. Saltveit SJ, Bremnes T, Linda OR. Effect of sudden increase in discharge in a large river on newly emerged Atlantic salmon (*Salmo salar*) and brown trout (*Salmo trutta*) fry. Ecol Freshw Fish. 1995;4:168–74.

Publisher's note